ELSEVIER

Ceramics International 33 (2007) 395–399

CERAMICS INTERNATIONAL

www.elsevier.com/locate/ceramint

Processing and piezoelectric properties of porous PZT ceramics

Tao Zeng *, XianLin Dong, ShuTao Chen, Hong Yang

Shanghai Institute of Ceramics, Chinese Academy of Sciences, 1295 DingXi Road, Shanghai 200050, PR China

Received 4 July 2005; received in revised form 30 August 2005; accepted 29 September 2005
Available online 6 January 2006

Abstract

5–45% porous lead zirconate titanate (PZT) ceramics were fabricated by adding pore formers such as polymethyl methacrylate (PMMA) and dextrin and sintering at 1200 °C for 2 h. The optimum heating procedure was decided according to the thermogravimetric analysis of pore formers. The effects of different pore formers and their content on the microstructure and piezoelectric properties were investigated. With an increase in the content of pore formers, the porosity of sintered ceramics increased, which led to reduced dielectric constant (ε_{33}) and longitudinal piezoelectric coefficient (d_{33}) as well as enhanced hydrostatic piezoelectric voltage coefficient (g_h) and hydrostatic figures of merit ($d_h\, g_h$). The hydrostatic figures of merit ($d_h\, g_h$) of 41% porous PZT were 10 times more than that of 95% dense PZT.

Keywords: B. Porosity; C. Piezoelectric properties; C. Hydrostatic figures of merit; D. PZT

1. Introduction

Lead zirconate titanate (PZT) is an important piezoelectric material which has been largely used in ultrasonic transducers for applications like hydrophones, underwater transducers, actuators, biomedical imaging etc [1–5]. However, dense piezoceramic materials such as dense PZT possess low piezoelectric response and poor acoustic matching between the ceramics and the media due to the great difference in density. The hydrostatic figure of merit, $d_h\, g_h$, is defined to evaluate the effect of a pizeoceramic used as underwater acoustics [6–9]. The hydrostatic piezoelectric voltage coefficient, g_h, can be calculated by d_h/ε. As the dielectric constant decreases, the g_h increases, so the figure of merit increases. One of the possibilities to lower the dielectric constant is the incorporation of void space into the dense PZT samples. Furthermore, an increase in the amount of porosity leads to a decrease in the transverse piezoelectric coefficient ($-d_{31}$) relative to the longitudinal one (d_{33}) [10], which produces an increase in the hydrostatic strain coefficient, d_h ($=d_{33} + 2d_{31}$), so that higher electrical charges are generated per unit hydrostatic force. Moreover, the difference in acoustic impedance of the piezoelectric and the ambient medium (such as air or water) determines the reflection and transmission of sound energy at the interface [11]. The closer the impedances are between each other, the less sound energy is reflected at the interface. This can be possibly achieved by adjusting the number of pores to reduce the sound velocity and impedance values to close water or air [12,13]. Porous PZT with different pore size and porosities can be made by burning pore formers with different sizes and contents such as starch [14,15], PVA [16], PVB [17], yeast [18], during the sintering process. The purpose of this work is to investigate the effects of different pore formers and their content on the microstructure and piezoelectric properties of porous PZT ceramics.

2. Experiment procedure

2.1. Sample preparation

Porous PZT ceramics were prepared by mixing PZT powder with pore formers. The designed compositions of mixed powders were $Pb(Zr_{0.53}Ti_{0.47})O_3$ + 0.5 wt.%Nb_2O_5 + αPMMA and $Pb(Zr_{0.53}Ti_{0.47})O_3$ + 0.5 wt.%Nb_2O_5 + βdextrin, respectively, where $\alpha = 0$, 2.5, 5, 10, and 12.5 wt.%, $\beta = 0$, 3, 6, 9, 12, 15, and 18 wt.%. The size of PMMA was controlled between 120 μm and 170 μm while the size of dextrin was in the range of 20–40 μm. The weighted powders for the designated PZT composition were ball milled for 6 h with zirconia balls as the grinding media and alcohol as the solvent. After milling, the slurry was dried at room temperature and then

* Corresponding author. Tel.: +86 21 52412009; fax: +86 21 52413903.
E-mail address: zengtao@mail.sic.ac.cn (T. Zeng).

0272-8842/$32.00
doi:10.1016/j.ceramint.2005.09.022

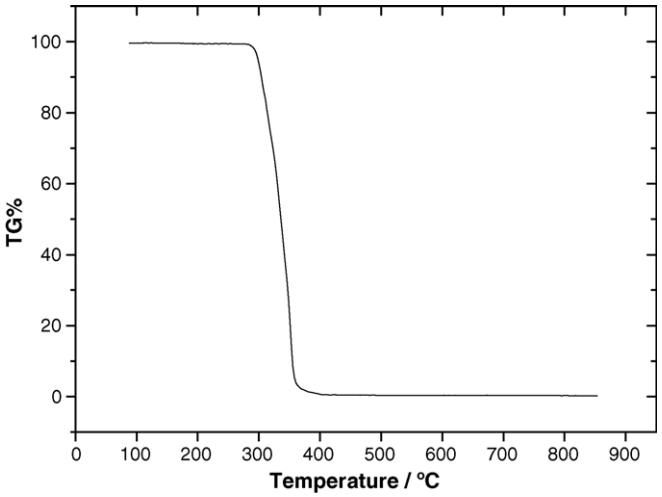

Fig. 1. TG curve of PMMA at a heating rate of 10 °C/min.

the powders were mixed with 5 wt.% PVA liquid addition. The mixed powder was pressed at about 200 MPa to ϕ 16 mm disks. From the thermogravimetric analysis of PMMA shown in Fig. 1, the optimum heating procedure was decided to begin with an initial heating rate of 120 °C/h up to 240 °C followed by 60 °C/h up to 420 °C and then 120 °C/h up to 850 °C to assure the complete burn out of the PMMA. Fig. 2 shows that dextrin begin to volatilize at 240 °C and completely burn out at 540 °C. Therefore the heating rate was initially 120 °C/h up to 240 °C, then 60 °C/h up to 540 °C and finally 120 °C/h up to 850 °C to assure the complete burn out of the dextrin. The compacts were sintered at 1200 °C for 120 min in soaking furnace. All the compacts were placed in a covered alumina crucible pitted with $Pb(Zr_{0.53}Ti_{0.47})O_3$ powders to reduce the volatilization of Pb. The sintered samples were ground to remove the surface layers, evaporated with silver electrodes in vacuum, and poled by applying a DC field of 3–4 kV/mm for 10 min in a silicone oil bath at 120 °C. Bulk density (ρ_b) was determined by the Archimedes method, and the porosity of sample was calculated from the ratio of the bulk density to the theoretical density (ρ_t = 8.02 g/cm^2).

2.2. Sample characterization

The sintered samples were analyzed by X-ray diffraction (Rigakv RAX-10) and the microstructures of porous PZT ceramics were observed by optical microscopy (TOTA-500III). The piezoelectric charge coefficient (d_{33}) was measured by a direct method based on a Quasi-static d_{33}-meter. The static capacitance (at 1 kHz), the dissipation factor tan δ and the electrical impedance as a function of frequency were measured by using an HP-4294A impedance bridge. The electromechanical coupling factors and transverse piezoelectric coefficient were determined from the values of resonance and antiresonance frequencies, density, dimensions and dielectric constant. The parameters of d_h, g_h and $d_h g_h$ were calculated from the measured d_{33}, d_{31} and ε_{33} values and the equations discussed in the introduction.

3. Results and discussion

3.1. Microstructure and mechanical properties

Fig. 3 shows the XRD patterns of the PZT, PZT–dextrin and PZT–PMMA ceramics sintered at 1200 °C for 2 h. It is noted that single perovskite structure were exhibited for all the sintered ceramics. No other phase was detected. The variations of porosity with the content of pore formers is shown in Fig. 4. The porosity increased with an increase in the content of pore formers at a fixed sintering temperature. Fig. 5 shows typical optical micrographs of both PMMA porous PZT ceramics and dextrin porous PZT ceramics with low and high porosities sintered at 1200 °C. It can be seen that for all the porous materials, macropores were formed in the ceramics after sintering. For the PZT ceramics with high porosity, some small pores incorporated into larger pores, and the pore sizes in porous PMMA ceramics were larger than porous dextrin ceramics. As the content of the PMMA increased, the porosity also increased, showing that the porosity and pore sizes are determined by the content and sizes of pore formers. It is shown

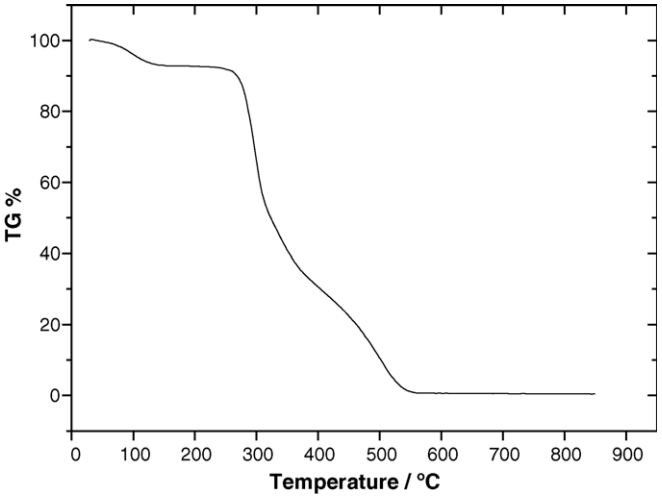

Fig. 2. TG curve of dextrin at a heating rate of 10 °C/min.

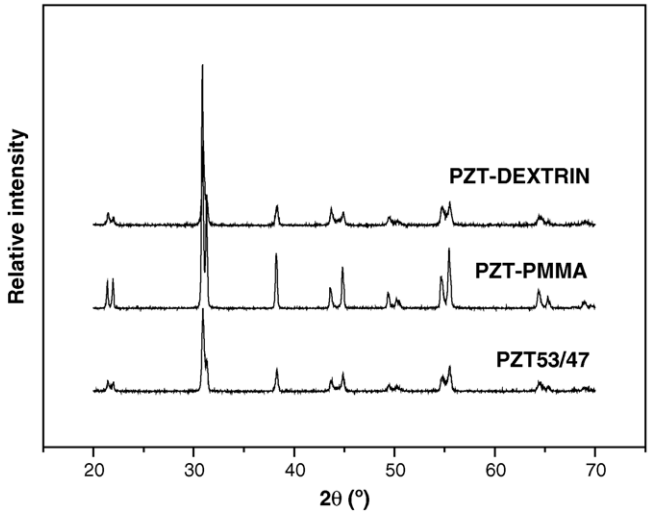

Fig. 3. XRD patterns of the PZT ceramics with different pore formers.

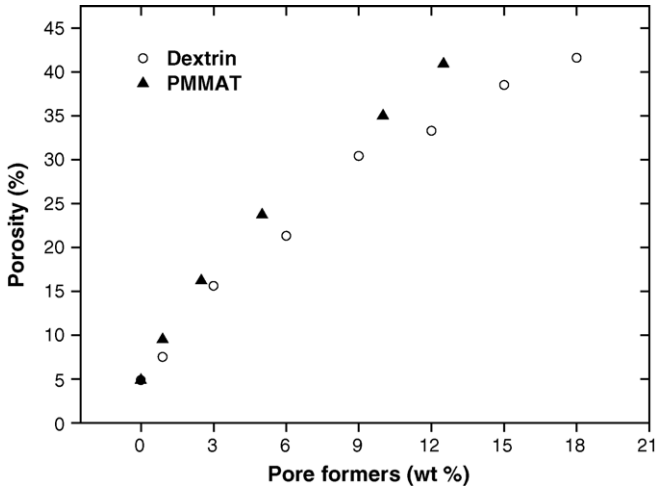

Fig. 4. Variation of porosity with the content of pore formers.

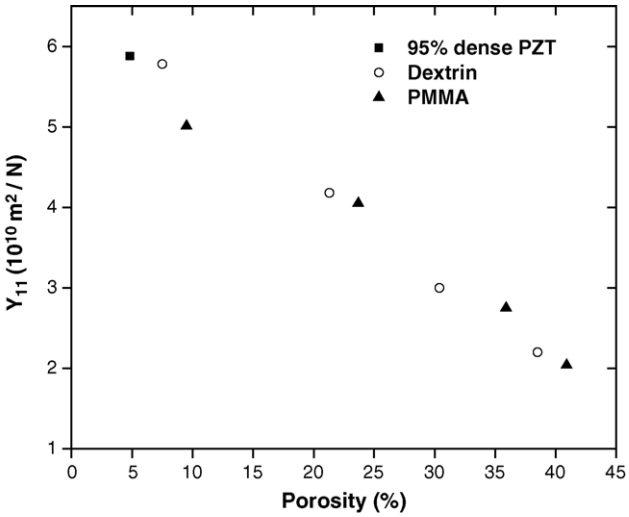

Fig. 6. Variation of Young's modulus of porous PZT ceramics with porosity.

in Fig. 6 that increased porosity led to a decrease in the Young's modulus.

3.2. Piezoelectric properties

The changes in piezoelectric coefficient and relative dielectric constant with porosity are shown in Figs. 7 and 8, respectively. The decrease in piezoelectric coefficient and relative dielectric constant with porosity for both PMMA and dextrin ceramics was greater than expected by considering only the volume fraction of pores, with zero piezoelectric coefficient and relative constant, within the ceramics. As for the observation from Carroll and Holt [19], the enhanced stress near the pores leads to an increase in microscopic stress and strain, which indicates an increased stress due to an increased volume fraction of pores in the porous PZT ceramics. There are two ways in which an increased stress can affect piezoelectric coefficient. One is by inhibiting the movement of domain walls and increasing depolarizing factors. The second one is by preventing grain growth and decreasing grain size. As the grain size decreases, the domain walls are inhibited to move because the increased grain boundaries contribute additional pinning points for the moving walls [20]. The relative dielectric constant, ε, is given by

$$\varepsilon_{\text{app}} = \frac{(1-p)(\varepsilon_{\text{sl}}-1)}{1+N_i(\varepsilon_{\text{sl}}-1)}$$

where ε_{app} is dielectric constant of samples with pores, ε_{sl} the dielectric constant of samples without pores, p is volume

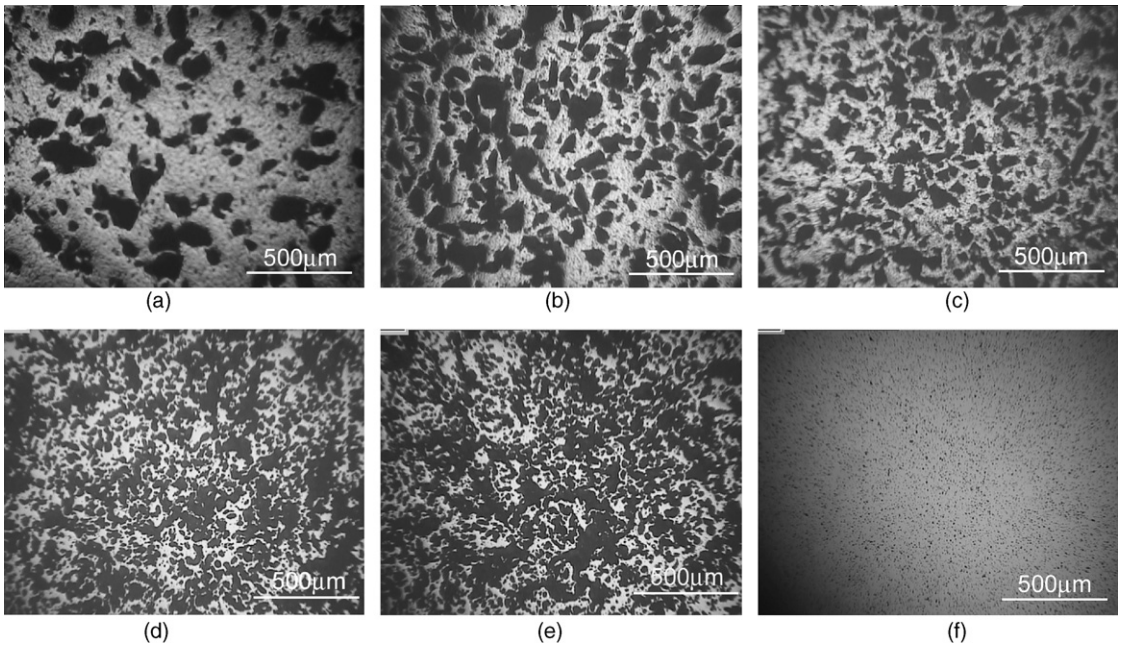

Fig. 5. Optical micrographs of porous piezoelectric materials (×120). (a) PZT with 5 wt.% PMMA, porosity, 24%. (b) PZT with 10 wt.% PMMA, porosity, 35%. (c) PZT with 12.5 wt.% PMMA, porosity, 41%. (d) PZT with 12 wt.% dextrin, porosity, 33%. (e) PZT with 21 wt.% dextrin, porosity, 46%. (f) PZT with 0% pore formers, porosity, 5%.

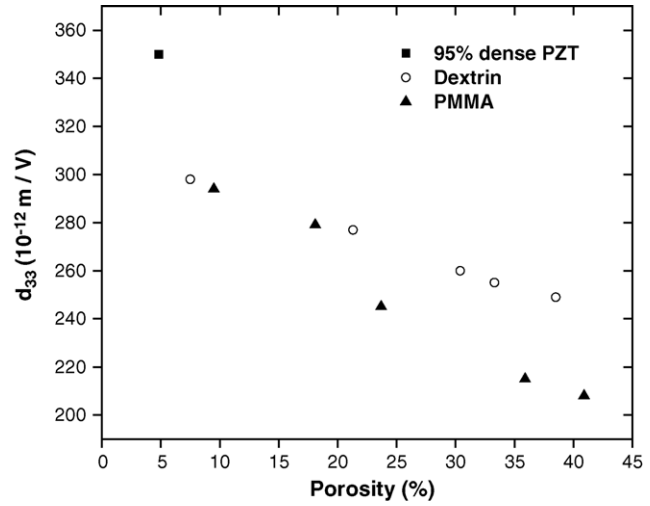

Fig. 7. Variation of longitudinal piezoelectric coefficient of porous PZT ceramic with porosity.

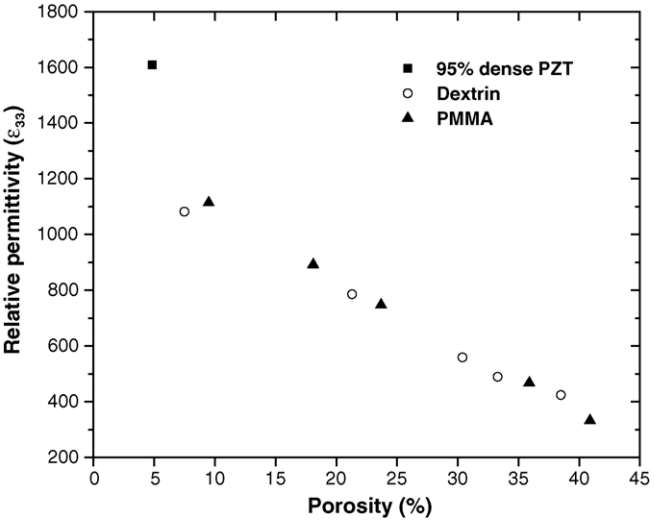

Fig. 8. Variation of relative dielectric constant of porous PZT ceramics with porosity.

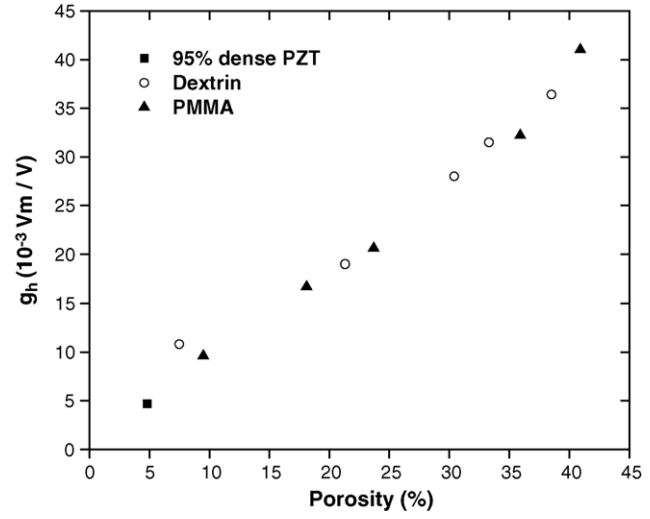

Fig. 9. Variation of hydrostatic piezoelectric voltage coefficient of porous PZT ceramics with porosity.

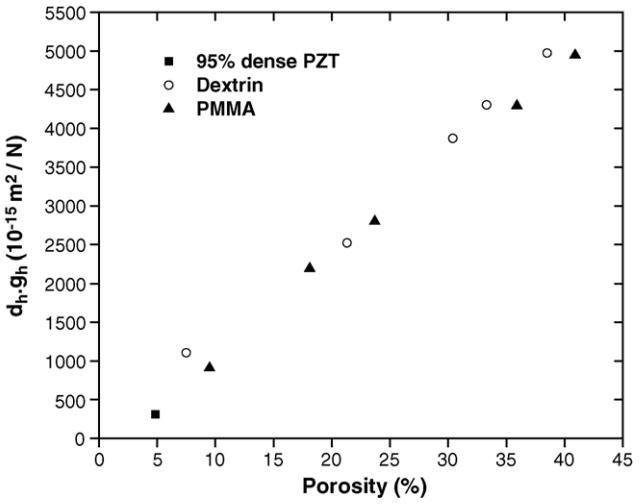

Fig. 10. Variation of hydrostatic figure of merit of porous PZT ceramics with porosity.

fraction of porosity and N_i are the depolarizing factors [21]. The depolarizing factors are consistent with an increased stress and strain for samples with higher porosity [22]. If the effect of depolarizing factors on dielectric constant were not accounted in, as the porosities increased, a linear decrease in dielectric constant should occur. However, the porosity increased, and then the depolarizing factor (N_i) rose, which caused a further decrease in dielectric constant.

The reduced $-d_{31}$ coefficient and lower dielectric constant of the porous PZT ceramics led to an increase in hydrostatic voltage constant (g_h), and large improvements are observed for both PMMA and dextrin ceramics when compared to 95% dense PZT, as seen in Fig. 9 The hydrostatic figure of merit ($d_h\, g_h$) shown in Fig. 10 increased with the amount of porosity up to over 10 times as compared with that of 95% dense PZT.

4. Conclusions

Porous PZT piezoelectric ceramics have been manufactured by using different pore formers (PMMA, dextrin) and sintered at 1200 °C over a range of porosity (5–45%). The porosity increased with an increase in the content of pore formers and the increased porosity led to a decrease in the Young's modulus. For the PMMA and dextrin based PZT ceramics, no significant differences in properties were observed even though their pore sizes are different. In the range of porosity, an increase in porosity lead to a decrease in d_{31} and $\varepsilon_{33,}$ for all the porous PZT ceramics, which resulted in improved g_h and $d_h\, g_h$ when compared to 95% dense PZT. The hydrostatic figures of merit ($d_h\, g_h$) of 41% porous PZT increased by over 10 times as compared with that of 95% dense PZT.

References

[1] R.Y. Ting, Piezoelectric properties of a porous PZT ceramic, Ferroelectrics 65 (1985) 11–20.
[2] T. Arai, K. Ayusawa, H. Sato, T. Miyata, K. Kawamura, K. Kobayashi, Properties of hydrophone with porous piezoelectric ceramics, Jpn. J. Appl. Phys. 30 (9B) (1991) 2253–2255.

[3] K. Mizumura, Y. Kurihara, H. Ohashi, S. Kumamoto, K. Okuno, Porous piezoelectric ceramic transducer, Jpn. J. Appl. Phys. 39 (9B) (1991) 2271–2273.
[4] S. Kumamoto, K. Mizumura, Y. Kurihara, H. Ohhashi, K. Okuno, Experimental evaluation of cylindrical ceramic tubes composed of porous Pb(Zr, Ti)O_3 ceramics, Jpn. J. Appl. Phys. 30 (9B) (1991) 2292–2294.
[5] J.F. Li, T. Kenta, O. Masaru, P. WEi, W. Ryuzo, Fabrication and evaluation of porous piezoelectric ceramics and porosity-graded piezoelectric actuators, J. Am. Ceram. Soc. 86 (7) (2003) 1094–1098.
[6] L. Martin, Dunn, T. Minoru, Electromechanical properties of porous piezoelectric ceramics, J. Am. Ceram. Soc. 76 (7) (1993) 1697–1706.
[7] L.V. Gibiansky, S.T. Toruato, On the use of homogenization theory to design optimal piezocomposites for hydrophone applications, J. Mech. Phys. Solids 45 (5) (1997) 689–708.
[8] C. Galassi, E. Roncari, C. Capiani, G. Fabbri, et al., Processing of porous PZT materials for underwater acoustics, Ferroelectrics 268 (2002) 47–52.
[9] C.R. Bowen, A. Perry, A.C.F. Lewis, H. Kara, Processing and properties of porous piezoelectric materials with high hydrostatic figures of merit, J. Eur. Ceram. Soc. 24 (2004) 541–545.
[10] S. Geis, J. Fricke, P. Lobmann, Electrical properties of PZT aerogels, J. Euro. Ceram. Soc. 22 (2002) 1155–1161.
[11] M.J. Creedon, W.A. Schulze, Axially distorted 3-3 piezoelectric composites for hydro-phone applications, Ferroelectrics 153 (1994) 333–339.
[12] G. Suyal, N. Setter, Enhanced performance of pyroelectric microsensors through the introduction of nanoporosity, J. Eur. Ceram. Soc. 24 (2004) 247–251.
[13] F. Craciun, G. Guidarelli, C. Galassi, E. Roncari, Elastic wave propagation in porous piezoelectric ceramics, Ultrasonics 36 (1998) 427–430.
[14] O. Lyckfeldt, J.M.F. Ferreira, Processing of porous ceramics by 'starch consolidation', J. Eur. Ceram. Soc. 184 (1998) 134–140.
[15] J.G. Kima, Y.J. Kwon, J.H. Ohb, et al., Sintering behavior and electrical properties of porous (Ba,Sr)(Ti,Sb)O_3 ceramics produced by adding cornstarch, Mater. Chem. Phys. 83 (2004) 217–221.
[16] W.J. Chao, K.S. Chou, Studies on the control of porous properties in the fabrication of porous supports, Key Eng. Mater. 113 (1996) 93–108.
[17] D.M. Liu, Control of pore geometry on influencing the mechanical property of porous hydroxyapatite, J. Mater. Sci. Lett. 15 (1996) 419–421.
[18] W.G. Chi, D.L. Jiang, Z.G. Huang, S.H. Tan, Sintering behavior of porous SiC ceramics, Ceram. Int. 30 (2004) 869–874.
[19] M.M. Carroll, A.C. Holt, Static and dynamic pore-collapse for ductile porous materials, J. Appl. Phys. 43 (4) (1972) 1626–1635.
[20] H.T. Martirena, J.C. Burfoot, Grain-size effects on properties of some ferroelectric ceramics, J. Phys. C: Solid State Phys. 7 (1974) 3182–3192.
[21] O. Kiyoshi, Recent developments in piezoelectric ceramics in Japan, Ferroelectrics 35 (1981) 173–178.
[22] A.T. Bruce, Y. Pin, H.G. John, et al., Pressure-induced phase transformation of controlled porosity Pb($Zr_{0.95}Ti_{0.05}$)O_3 ceramics, J. Am. Ceram. Soc. 84 (6) (2001) 1260–1264.